J. Braz. Chem. Soc., Vol. 8, No. 4, 357-362, 1997.
Printed in Brazil.

0103 - 5053 $6.00 + 0.00

Article

Studies of the Electrodeposition of Cobalt on a Vitreous Carbon Electrode

Rodnei Bertazzoli, and Maria de Fátima Brito Sousa

Universidade Estadual de Campinas, Departamento de Engenharia de Materiais/Fem, C.P. 6122 13083-970 Campinas - SP, Brazil

Received: July 10, 1996

Neste trabalho foram feitos experimentos usando técnicas de voltametria cíclica e pulso de potencial para o estudo do mecanismo de deposição do cobalto em meio de sulfato. A voltametria cíclica mostrou dois picos de dissolução, o que foi atribuído à dissolução de uma fase rica em hidrogênio e outra do metal quase puro. A análise cinética das curvas I-E na varredura reversa mostraram que, para uma solução com 0,37 M Co(II) e pH 6, o potencial de equilíbrio do par Co/Co(II) é -0,58 V *vs.* SCE e a corrente de troca, $I_o = 4{,}8 \times 10^{-6}$ A cm^{-2}. Os experimentos de pulso de potencial mostraram que o depósito de cobalto sobre o eletrodo de carbono vítreo apresenta nucleação progressiva seguido de crescimento tridimensional. Ambas as técnicas confirmaram que a deposição do cobalto acontece em duas etapas, com a transferência de um elétron cada.

Experiments of cobalt deposition on a vitreous carbon electrode were carried out using cyclic voltammetry and potential steps techniques, in a sulfate medium. Cyclic voltammetry showed two stripping peaks that were attributed to the dissolution of two phases: a hydrogen rich cobalt phase and a bulk cobalt phase. Kinetic analysis of I-E response on the reverse scan for a 0.37 M of Co(II), pH 6, presented a value of -0.58 V *vs.* SCE for the equilibrium potential of the Co/Co(II) couple. The exchange current density was estimated as $I_o = 4.8 \times 10^{-6}$ A cm^{-2} in this solution. Potential step experiments showed that the cobalt deposit on vitreous carbon is formed by a mechanism of progressive nucleation followed by 3-D growth. Both techniques confirmed that cobalt deposition takes place in two single electron steps.

Keywords: *cobalt deposition, nucleation of electrodeposits, cyclic voltammetry*

Introduction

Electrodeposited cobalt and cobalt based alloys are widely employed as hard protective coatings and as recording media in the computer industry. Cobalt has been deposited mainly from sulfate electrolytes, although studies in $CoCl_2$ and $Co(NH_4)_2(SO_4)_2$ based electrolytes can be found in the literature[1-4].

Mechanical properties and perpendicular magnetic anisotropy of cobalt films appear to be a function of the structure of the deposits, which depends on the pH of the solution and the conditions selected for depositing, such as temperature and current density[5-7]. However, the mechanism of cobalt reduction and the nucleation/growth process has received little attention, and it appears to be the key for a better understanding of the deposition process and for producing films with the required properties.

In this paper, cyclic voltammetry, hydrodynamic voltammetry and potential step techniques are used in order to identify the mechanism of cobalt reduction in a sulfate medium.

Experimental

The experiments were carried out in a three compartment cell. The working electrode and the Pt gauze counter electrode were separated by a glass frit, and a saturated calomel reference electrode (SCE) was mounted within a Luggin capillary. The working electrode was a vitreous carbon disc (A = 0.125 cm^2) which entered the cell from the top, so that the surface of the disc was horizontal. In the

hydrodynamic experiments it was rotated in the range from 400 to 2500 rpm.

The electrolytic solutions were prepared from tridistilled and deionized water and analytical grade reagents. All experiments were carried out using 0.5 M sodium sulfate and 0.5 M boric acid as a supporting electrolyte. Cobalt was added as $CoSO_4.7H_2O$ (Merck) at the required concentration for each experiment. Sulfuric acid or sodium hydroxide was used for adjusting the pH.

The electrochemical experiments were controlled in a 273A Potentiostat coupled with a 616 Rotating Disc Electrode, both controlled by a 270 Research Electrochemical Software, all from EG&G PARC. All experiments were performed at room temperature, and the electrolytes were thoroughly purged with nitrogen.

Results and Discussion

Cyclic voltammetry

Figure 1 shows voltammograms recorded for a 0.37 M Co(II), pH 4.4 solution on a vitreous carbon electrode. The potential was scanned from 0.0 V *vs.* SCE to more negative values of -0.98, -1.00, -1.02 and -1.04 V, at a scan rate of 20 mV s^{-1}. Then, the direction of scanning was reverted to the initial value of the potential.

On the forward scan almost no current was observed until the potential reached -0.95 V. Thereafter, the cathodic current increased rapidly once the nucleation process began. When the direction of the potential scan was reverted a current maxima was observed due to the rise of the surface area in the early stages of the nucleation process, before coalescence of the growing nuclei[4]. As the lower limit was shifted more negatively or as the potential scan rate was decreased, this effect was no longer observed. The current densities were higher on the reverse scan until the response reached zero current at -0.60 V.

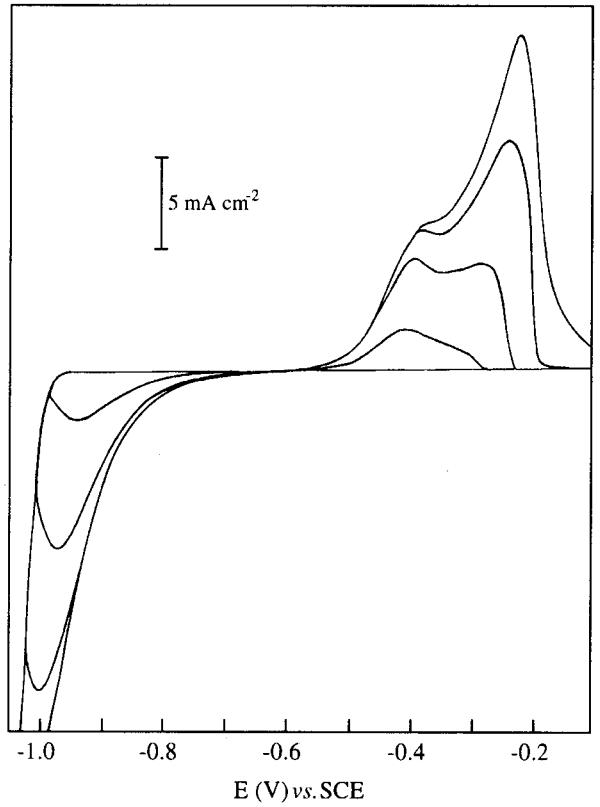

Figure 1. Voltammograms recorded at 20 mV s^{-1} for a 0.37 M Co(II) solution, pH 4.4, on a vitreous carbon electrode.

The voltammograms from Fig. 1 present many characteristics of a metal reduction reaction, particularly the "nucleation loop" towards the negative limit and the dissolution peaks on the reverse scan. When the lower limit was extended, the cathodic current continued rising to 60 mA cm^{-2} (at -1.10 V) from which a peeling tendency was observed.

The I-E responses from Fig. 1 also show, as common features, two stripping peaks on the reverse scan, at -0.40 and -0.25 V, when only one was expected. The existence of more than one peak during dissolution of a single metal can be interpreted in many ways. This fact has been considered in the literature as a) dissolution of an underpotential deposited phase[8], b) differences in the crystal lattice orientation[5], c) passivation due to metal oxide/hydroxide formation[9-11] or d) dissolution of a codeposited hydrogen rich metallic phase preceding the dissolution of the bulk phase[12]. All these interpretations have their drawbacks and present difficult experimental confirmation. If we consider the stripping peaks in the voltammograms from Fig. 1, the charge of the second peak is too great to be related to an underpotential deposited phase dissolution. Passivation can be disregarded since the peak currents of dissolution increase with the charge of deposition. Visual observations of the deposits showed reliable reflectance and brightness and no oxides/hydroxides were detected on the electrode surface during dissolution, once the deposits were still reflective.

Figure 2 shows three voltammograms obtained in a 0.37 M Co(II) solution at different pH values (2.8, 4.4 and 6.0). For the pH 4.4 solution the same two peaks (at -0.40 and -0.25 V) are observed. However, for the pH 2.8 solution, the voltammogram shows only the first peak at -0.40 V. Increasing the pH to 6.0, only the second peak can be seen.

In lieu of these findings a new test was carried out. A series of depositions at constant potential was made in a pH 2.8 solution and 90 mC cm^{-2} of cobalt was deposited at -1.00 V. Then, the deposits were dissolved by scanning the potential range from -0.6 to 0.0 V at, 20 mV s^{-1}, after different times resting, at open circuit potential, in the solution of deposition. The result of this operation is depicted in Fig. 3 which shows stripping peaks of a fresh cobalt film (marked as **A**) and of a 30 min. rested deposit (peak **B**).

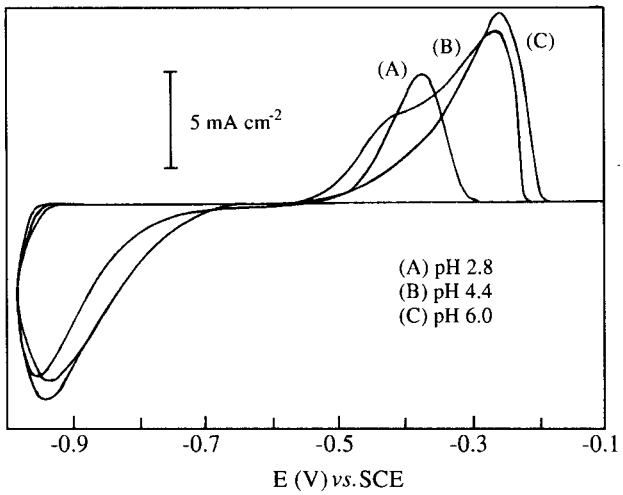

Figure 2. Voltammograms recorded at 20 mV s^{-1} for a 0.37M Co(II) solution and pH (A) 2.8, (B) 4.4 and (C) 6.0.

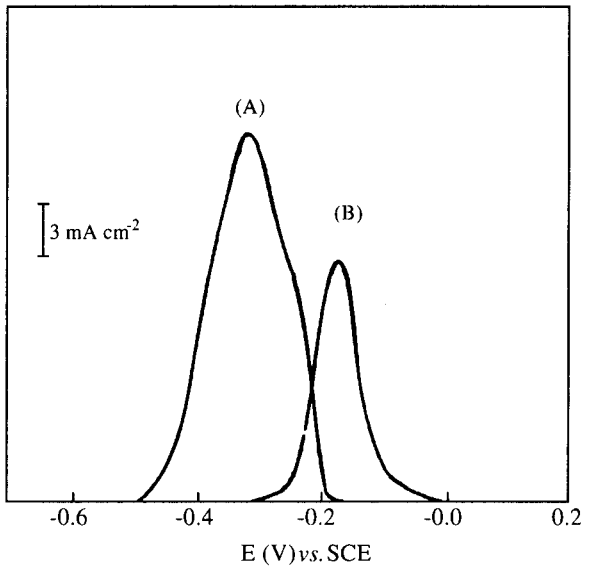

Figure 3. Stripping peaks of 150 mC cm^{-2} of cobalt deposited at -0.95 V *vs.* SCE. Dissolution of a (A) fresh film and (B) 30 min rested deposit. Solution of 0.37 M Co(II), pH 2.8.

Considering the behavior of the stripping peaks in Figs. 2 and 3 we can associate the first peak with the dissolution of a hydrogen rich phase. The potential shift of the dissolution peak in Fig. 3 shows that the rest may lead to a partial conversion of the H-rich phase into pure cobalt or bulk phase. This has already been observed for nickel[12], and high levels of internal stress in cobalt layers has been reported due to hydrogen codeposition[13].

Kinetic parameters

The 0.37 M Co(II) solution at pH 6, was used for depositing 5 mC cm^{-2} of cobalt in order to coat the electrode surface. Then the potential was scanned from -0.95 to 0.0 V at 5mV s^{-1}. The I-E data obtained in this operation can be regarded as the response for the Co/Co(II) couple on a freshly deposited cobalt surface. In the absence of significant competing reactions, the zero current potential is a good estimate of the equilibrium potential for the Co/Co(II) couple, and the shape of the I-E characteristic reflects the kinetics of the metal/metal ion couple. In an earlier paper we found -0.61 V for the equilibrium potential of the Co/Co(II) couple[14]. The I-E response of this reverse scan obtained on the fresh cobalt surface is depicted by the Tafel plot in Fig. 4 where well-defined Tafel regions are observed over two orders of current density magnitude. The cathodic and anodic slopes of the linear portion of the curves are 1/120 and 1/58 mV, respectively. The first value is characteristic for a reduction reaction of bivalent metals which occurs in two single electron steps, but the latter is not the expected value. If reduction takes place in single electron steps, *i.e.*

$$Co^{2+} + e^- \rightleftharpoons Co^+ \quad (1)$$

$$Co^+ + e^- \rightleftharpoons Co \quad (2)$$

the overall rate of conversion of Co(II) to cobalt metal is determined by the kinetics of the Co(II)/Co(I) couple involving the transfer of a single electron, assuming that Reaction 2 is the rapid step. The Tafel slope in this case is 1/120 mV. The overall reaction rate of Co to Co(II) oxidation must be determined by the kinetics of the same couple. The rate of oxidation is given by

$$I = Fk\,[Co^+]_{x=0} \quad (3)$$

where **k** is the potential dependent rate constant for the oxidation of Co(I) to Co(II) at the electrode surface, and $[Co^+]_{x=0}$ is the concentration of Co(I) at the electrode surface. The concentration of Co(I) can be found assuming that the rapid step is in equilibrium. Then, the Nernst equation may be applied to Reaction 2, *i.e.*,

$$E_e = E^0_e + \frac{2.3\,RT}{F}\log[Co^+] \quad (4)$$

and used to estimate the concentration of Co(I) at the surface. Hence, Eq. 3 becomes

$$\log I = constant + \frac{(1+\alpha)F}{2.3\,RT}\,\eta \quad (5)$$

If $\alpha = 0.5$, the Tafel slope is 1/40 mV. This is not the value calculated for this experiment probably due to the competing dissolution of the hydrogen rich phase.

The intercept of the straight lines from Fig. 4 showed an equilibrium potential of -0.58 V which is a more accurate estimate for the Co/Co(II) couple, and corresponds well with the calculated value[15]. From Fig. 4 the exchange current was then estimated as $I_o = 4.8 \times 10^{-6}$ A cm^{-2}.

In the hydrodynamic voltammetry on a rotating vitreous carbon electrode the concentration of Co(II) in the electro-

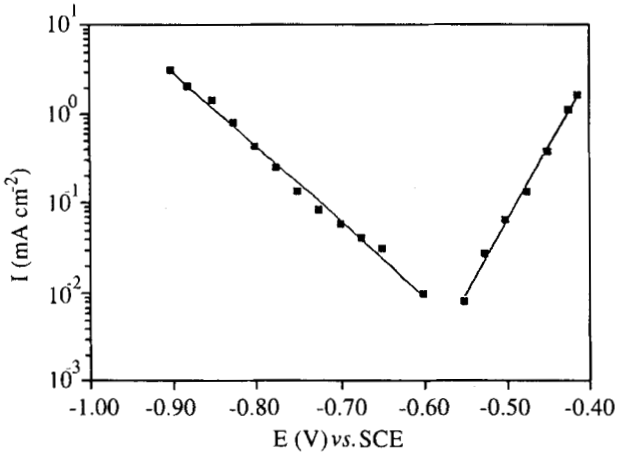

Figure 4. Tafel plot of the I-E response obtained on the reverse scan at 5 mV s^{-1} for a solution with 0.37 M of Co(II), pH 6.0.

lyte was reduced to 3.7 mM and the pH adjusted to 6.0. Then, a new set of voltammograms was recorded using rotation rates of 400, 900, 1600 and 2500 rpm (Fig. 5). All the main features of those I-E curves have been described earlier, excluding the fact that they present plateaus of mass transport controlled cathodic current. For all voltammograms the charge ratio was in the range from 0.88 to 0.92. Figure 5 presents the cathodic portions of the curves showing the plateaus of mass transport controlled currents. The values of limiting currents, taken at -1.18 V, are plotted versus the square root of the rotation rates at the right side of Fig. 5. The linear dependence between both parameters fit the Levich equation well, revealing a mass transport controlled reduction reaction. Considering the kinematics viscosity as $\nu = 10^{-2}$ cm^2 s^{-1}, the diffusion coefficient of Co(II) species was estimated as $D = 4 \times 10^{-6}$ cm^2 s^{-1}, which

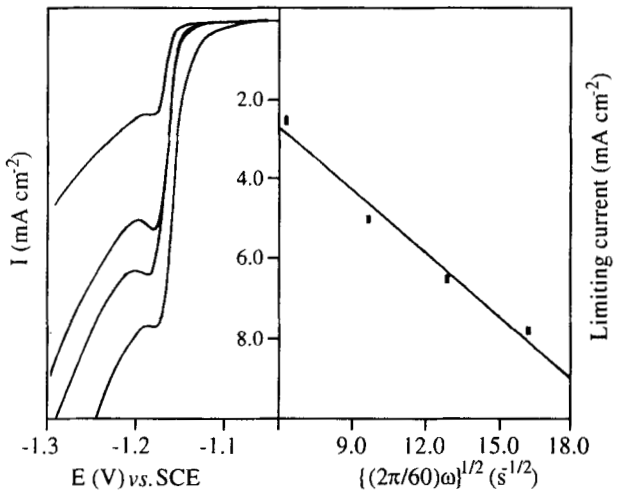

Figure 5. Left: Plateaus of mass transport controlled current density obtained on a rotating vitreous carbon disc electrode, at 20 mV s^{-1}. Solution with 3.7 mM of Co(II), pH 6.0. From the top the rotation rates are 400, 900, 1600 and 2500 rpm. Right: Levich plot of limiting current *vs.* square root of the rotation rates.

is in good agreement with the values found in the literature[16].

Potential step experiments

In the potential pulse experiments a 0.37 M Co(II) solution at pH 6.0 was used. In these experiments the potential was stepped from -0.60 V, where no electrode reaction occurs, to a value in the range of -0.95 to -1.10 V, and the current was recorded as a function of time. A set of I-t transients from such experiments are shown in Fig. 6. It may be seen that after an initial charging spike, the current drops to a value close to zero before increasing with time until it reaches a steady state value. Such transients are characteristics of nucleation and phase growth of a metal on the vitreous carbon surface, despite the fact that the existence of a maximum at higher potentials reveals a partially diffusion controlled process[17]. In this case hydrogen evolution amplifies the response without changing its shape.

Therefore, the early parts of the rising transients were analyzed by plotting I^n *vs.* t. Four cases are possible for the value of **n**: a) n = 1/2 for instantaneous nucleation and b) n = 1/3 for progressive nucleation when both are controlled by electron transfer. When the nucleation process is mass transport controlled, c) n = 2 for a instantaneous nucleation and d) n = 2/3 for the progressive process[17,18]. Figure 7 shows that good linear plots, presenting the best correlation coefficient for the linear regression, are obtained when n = 1/3, as predicted by the equation

$$I \cong \frac{n F k^3 \pi M^2 A}{\rho^2} t^3 \qquad (6)$$

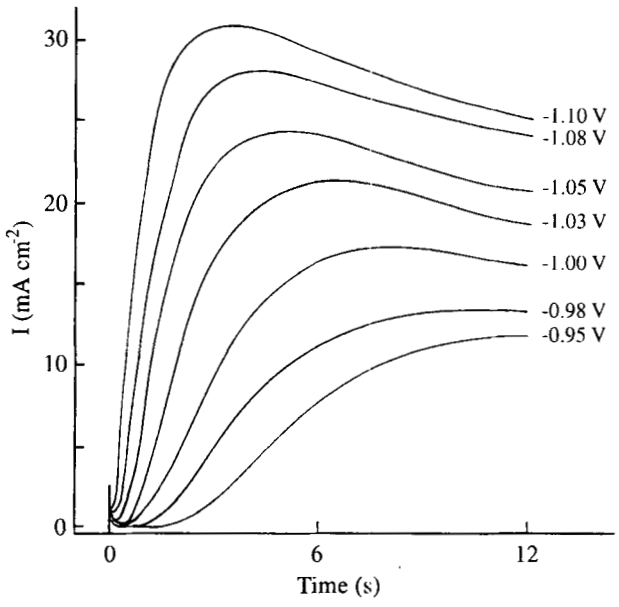

Figure 6. I-t transients in response to the step experiments from -0.58 V to the potential shown. Solution: 0.37 M of Co(II), pH6.0.

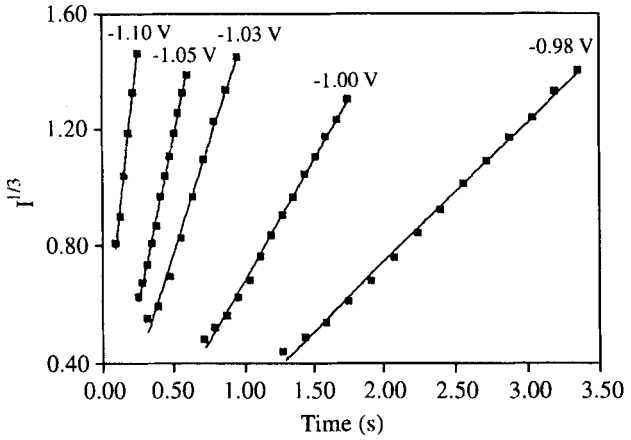

Figure 7. $I^{1/3}$ *vs.* t plot for the early stages of the nucleation process. Data taken from Fig. 6.

where **n** is the number of electrons involved in the overall electrode process, **F**, the Faraday constant, **k**, rate constant for growth, **M**, the molecular weight, **A**, rate constant for nucleation and ρ, density of the growing phase. The linear dependence between **I** and $\mathbf{t^3}$ indicates that the cobalt deposit is formed by a mechanism where progressive nucleation is followed by three-dimensional growth under electron transfer control in the early stages of the process.

A plot of the logarithm of the slopes of the $I^{1/3}$ *vs.* t plots against overpotential is also linear and has a slope of -1/124 mV as is seen in Fig. 8. The slope, which is proportional to $A^{1/3}k$, is shown to be a function of the potential. If we consider that the rate constant for nucleation (**A**) does not change meaningfully in the range of chosen potential, Eq. 6 can be written as:

$$\ln \frac{I^{1/3}}{t} = constant_1 + \ln k \qquad (7)$$

The rate constant for electron transfer is

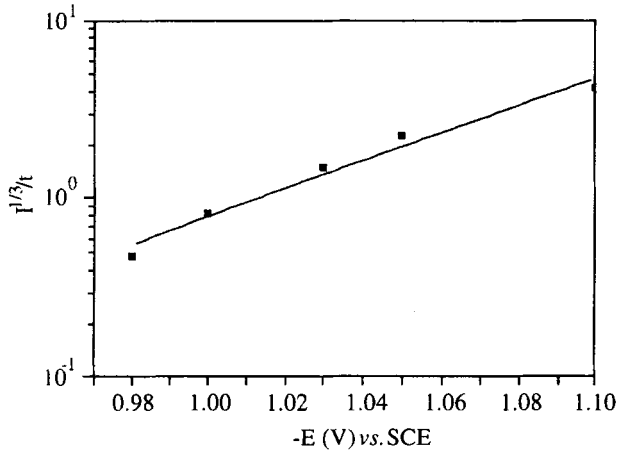

Figure 8. Plot of the logarithm of the slopes of the $I^{1/3}$ *vs.* t plot against potential. Data taken from Fig. 7.

$$k = k_0 \exp[\frac{\alpha n F}{RT}\eta] \qquad (8)$$

and, inserting Eq. 8 into Eq. 7, it is possible to write that

$$\ln \frac{I^{1/3}}{t} = constant_2 + \frac{\alpha n F}{RT}\eta \qquad (9)$$

Equation 9 shows how the slope from the plot ln ($I^{1/3}$/t) *vs.* η is proportional to the Tafel cathodic slope, and the slope obtained from Fig. 8 confirmed the early results from cyclic voltammetry. This is a new piece of evidence, *i.e.*, the cobalt reduction reaction probably takes place in two single electron steps.

Conclusions

The results reported here confirm that the cobalt deposition is possible in a buffered sulfate solution where cyclic voltammetry demonstrates that the deposition/dissolution of cobalt is a facile reaction, occuring without substantial overpotential . The competing hydrogen reduction rate is pH dependent. For lower pH, hydrogen formation is intense which leads to the nucleation of a hydrogen rich cobalt phase along the cobalt bulk phase. As the pH of the sulfate solution is increased, this effect is minimized, and the pure cobalt phase is preferentially formed.

I-E voltammograms obtained for 0.37 M Co(II) pH 6.0 solution, in steady state conditions, presented an equilibrium potential of -0.58 V and an exchange current density of 4.8 x 10^{-6} A.cm^{-2} . The cathodic Tafel slope extended to a two orders of current magnitude was found to be 1/120 in an initial finding of a two single electron step reduction reaction. By hydrodynamic voltammetry experiments on a rotating electrode the difusion coefficient was calculated as D = 4 x 10^{-6} cm^2 s^{-1}.

Potential step experiments showed that electrocrystalization of cobalt is progressive followed by tridimensional growth, once the plots of I *vs.* t^n , n = 1/3. The slope found in the plot of ln ($I^{1/3}$/t) *vs.* E was 1/124, confirming the results obtained from cyclic voltammetry which showed that the cobalt reduction reaction probably takes place in two single electron steps.

References

1. Morral, F.R.; Safranek, W.S. In *Modern Electroplating;* Lowenhein, F.A. ed., J. Willey and Sons, 1974, p. 152.
2. Lakshminarayanan, G.R.; Chen, E.S.; Sadak, J.C.; Sauter, F.K. *J. Electrochem Soc.* **1976**, *123*, 1612.
3. Cui, C.Q.; Jiang, S.P.; Tseung, A.C.C. *J. Electrochem. Soc.* **1990**, *137*, 3418.
4. Fletcher, S.; Halliday, C.S.; Gates, D.; Westcott, M.; Lwin, T.; Nelson, G. *J. Electroanal. Chem.* **1983**, *159*, 267.

5. Boltushkin, A.V.; Tochitskii, T.A.; Fedosyuk, V.M. *Elektrokhimiya* **1989**, *25*, 359.
6. Nakahara, S.; Mahajan, S. *J. Electrochem. Soc.* **1980**, *127*, 283.
7. Sard, R.; Schwarts, C.D.; Weil, R. *J. Electrochem. Soc.* **1966**, *113*, 424.
8. Jaya, S.; Rao, T.P.; Rao, G.P. *Electrochim. Acta* **1987**, *32*, 1073.
9. Bockris, J.O'M.; Drazic, D.; Despic, A.R. *Electrochim. Acta* **1961**, *4*, 325.
10. Sato, N.; Okamoto, G. *J. Electrochem. Soc.* **1964**, *111*, 897.
11. Heusler, K.E. *Ber. Bunsenges* **1967**, *71*, 620.
12. Fleishmann, M.; Saraby-Rentjes, A. *Electrochim. Acta* **1984**, *29*, 69.
13. Sotirova, G.; Sarnev, S.; Armyanov, S. *Electrochim. Acta* **1989**, *34*, 1237.
14. Bertazzoli, R.; Pletcher, D. *Electrochim. Acta* **1993**, *38*, 671.
15. Bard, A.J.; Parsons, R.; Jordan, J. In *Standard Potentials in Aqueous Solutions;* Marcell Dekker, NY, 1988.
16. Xiong, J.; May, P.M.; Ritchie, I.M. *Electrochim. Acta* **1987**, *32*, 1035.
17. Gunawardena, G.; Hills, G.; Montenegro, I.; Scharifker, B. *J. Electroanal. Chem.* **1982**, *138*, 225.
18. Greef, R.; Peat, R.; Peter, L.M.; Pletcher, D.; Robinson, J. In *Instrumental Methods in Electrochemistry;* Ellis Horwood Ltd., Chichester, 1985.

FAPESP helped in meeting the publication costs of this article